RSC Advances

PAPER

View Article Online
View Journal | View Issue

Cite this: *RSC Adv.*, 2016, **6**, 95067

The behavior of hydrophobic-core/hydrophilic-shell structured microgels at an interface: from Mickering emulsion to colloidosomes with dual-level controlled permeability†

Yi Gong, Mao Wang and Jianying He*

A bottom-up approach was employed to prepare colloidosomes with dual-level controlled permeability. Starting from the monodisperse poly-2,2,2-trifluoroethyl methacrylate (PTFMA) core, different sizes of microgels were obtained by introducing varying thicknesses of the poly(*N*-isopropylacrylamide-*co*-acrylic acid) (P(NIPAM-*co*-AAc)) shell. The effects of the core on the mechanical properties of the microgels and their behavior at the oil/water interface in a Mickering emulsion were carefully studied. The colloidosomes were then obtained by "locking" the interfacial microgels in the Mickering emulsion. The release of the model drug FITC-Dex from colloidosomes was examined in selected media and the controllable release of the drug was achieved by adjusting the pH (coarse level) and the ratio of the shell to core size in the microgels (fine level). The dual-level controlled permeability of the colloidosomes enabled the high precision that is necessary for the pH triggered drug release system. It is the first demonstration of the control of the permeability of colloidosomes that can be achieved by controlling the size of the shell and core of the microgels to the core hydrophobicity and the shell hydrophilicity. Both the convenience and precision of the control of the permeability of colloidosomes were improved in this way due to the mature size control technology in the microgel syntheses.

Received 17th July 2016
Accepted 22nd September 2016

DOI: 10.1039/c6ra18215a

www.rsc.org/advances

1 Introduction

Colloidosomes are hollow microcapsules with a wall composed of particles at the colloidal scale. Colloidosomes has received considerable attention due to their promising applications in drug delivery systems,[1] cell encapsulation,[2,3] biotechnology,[4] catalysis,[5–7] and sensors.[8] In general, colloidosomes are synthesized through the self-assembly of colloidal particles at the surface of emulsion droplets. These emulsions are named as Pickering emulsions or Mickering emulsion based on the fact that the colloidal particles are rigid particles[9] or microgels.[10] The colloidal particles tend to pack close together at the surface of the droplets in the emulsion to minimize the free energy of the system. A certain number of techniques, such as annealing,[9] polyelectrolyte complexation[3,11] and covalent cross-linking,[12,13] are capable of being applied to "lock" these particles for the formation of the wall of the microcapsules. Since the wall of the colloidosomes is composed of integrated colloidal particles, the functionality of the colloidal particles can be inherited by the as-formed colloidosomes[14] to meet practical requirements.

As one type of emerging colloidal particle, functional microgels have been explored in recent decades. Many investigations have been reported on the fabrication of colloidosomes using microgels.[10,12,15] Unlike rigid particles, microgels usually can be swollen in good solvents, giving them various functionalities such as thermal and pH sensitivity.[16] However, their poor mechanical properties are often accompanied by their excellent interaction with the solvents. It has been reported that soft microgels are easily deformed at the oil/water interface to minimize the free energy of the system.[10,17] As a result, the colloidosomes consisting of soft microgels have limited mechanical properties. To obtain robust microgels without sacrificing functionalities, researchers have investigated core–shell structured microgels, which consist of materials with different mechanical properties.[18–21] In this study, size tunable microgels with a rigid core of the poly-2,2,2-trifluoroethyl methacrylate (PTFMA) and a soft shell of poly(*N*-isopropylacrylamide-*co*-acrylic acid) (P(NIPAM-*co*-AAc)) were developed. PTFMA has a higher elastic modulus[18] than P(NIPAM-*co*-AAc) based particles.[19] The effects of the rigid core on the behavior of microgels were studied.

As vehicles for encapsulating and protecting sensitive molecules such as drugs and biologically relevant molecules, the permeability of colloidosomes is of crucial importance, which strongly depends on the colloidal particles forming their

Department of Structural Engineering, Faculty of Engineering Science and Technology, NTNU, Norwegian University of Science and Technology, 7491, Trondheim, Norway. E-mail: jianying.he@ntnu.no

† Electronic supplementary information (ESI) available: Zeta potentials of small, medium and large microgels against pH. See DOI: 10.1039/c6ra18215a

walls. Several efforts have been made to control the permeability of colloidosomes. San Miguel *et al.* introduced numerous methods including ethanol consolidation, polyelectrolyte deposition and incorporation of a hydrophobic polymer to control the capsule permeability. Each of these approaches led to a remarkable reduction in permeability without sacrificing the function of the triggered drug release.[20] Kim *et al.* developed colloidosomes by assembling the colloidal particles on the surface of temperature-responsive microgels. The permeability of as-formed colloidosomes can be adjusted by the size and elastic modulus of the colloidal particles.[15] It has been proven that the selectivity as well as the permeability of the colloidosomes can be controlled by tuning the size and functionality of the particles forming its wall.[21]

In general, the control of the size of the colloidal particles and the introduction of extra polyelectrolytes are the two commonly used methods to control the permeability of colloidosomes. In this study, we introduce a novel and effective method to control the permeability of colloidosomes based on the abovementioned core–shell structured microgels, schematically illustrated in Fig. 1. The PTFMA core of the microgels is hydrophobic,[22] whereas the shell is hydrophilic P(NIPAM-*co*-AAc). P(NIPAM-*co*-AAc) in the shell is a well-known pH sensitive polymer and its permeability can be markedly affected by pH.[23] As a result, pH changes can trigger the drug to be released by the synthesized colloidosomes. However, pH alone is not sufficient for the precise control of the release process, whereupon we demonstrated the fine-tuning of the permeability by manipulating the ratio of the shell to core size in the microgels used as the building blocks of colloidosomes. As shown in Fig. 1, the wall of colloidosomes is actually a hydrophilic matrix with hydrophobic particles embedded after the locking process. Due to their dramatic difference in hydrophobicity, the shell and core have different selectivities to the loaded molecules; therefore, the permeability of colloidosomes can be controlled by adjusting the fraction of the hydrophilic and hydrophobic parts in the microgels. The adjustment on permeability of colloidosomes is tantamount to size control on shell and core of microgels, thus both convenience and precision are improved. The designed colloidosomes with dual-level controllable permeability hold great promise in drug delivery applications. The proposed fabrication of colloidosomes from core–shell structured microgels also sheds new light on integrated multifunction for colloidosomes.

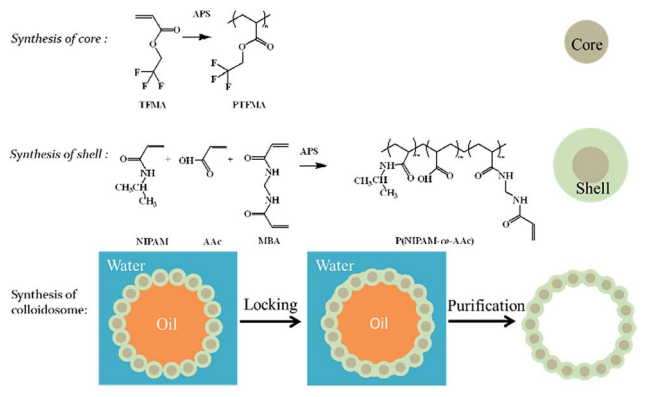

Fig. 1 Illustration of the synthesis of the core–shell microgels and the colloidosomes.

2 Experimental

2.1 Materials

2,2,2-Trifluoroethyl methacrylate (TFMA), *N*-isopropylacrylamide (NIPAM), *N*,*N*′-methylenebis(acrylamide) (MBA), acrylic acid (AAc), ammonium persulfate (APS), coumarin 7 (C7), nile red (NR), chitosan and fluorescein isothiocyanate–dextran (FITC-Dex, MW = 3000–5000) were purchased from Sigma Aldrich. Limonene (purity of 96%) was purchased from Fisher Scientific. All reagents were used as received. Millipore water with a resistivity of 15 MΩ cm was used as ultrapure water.

2.2 Synthesis and characterization of microgels

The surfactant-free polymerization synthesis procedure was developed based on the literature[24] after modification. The fluorescent core of microgels was synthesized by polymerization of TFMA. The fluorescent dye C7 (1.0 mg) was dissolved in 10.0 mL of TFMA. A 2 mL aliquot of this mixture was transferred into a three-neck round bottom flask and 72 mL of ultrapure water was added. After addition of 3 mL of APS solution (0.2000 g/100 mL), the reaction mixture was degassed in an argon flow environment. The temperature of the mixture was then increased to 70 °C for 2 hours for the core synthesis. Subsequently, 0.6250 g of NIPAM (81% mole ratio) and 0.0625 g (6% mole ratio) of the cross-linker MBA in 10 mL of ultrapure water and 5 mL of AAc (13% mole ratio) solution (1.25 mL/100 mL) were added into the reaction mixture for the formation of the shell while the temperature was maintained as 70 °C for 4 hours. After the reaction completed, the as-formed particle dispersion was purified by centrifugation and re-dispersed in ultrapure water 3 times. The P(NIPAM-*co*-AAc) microgels without a core–shell structure were synthesized based on the literature.[3]

The zeta-potential and hydrodynamic diameter of the microgels were measured by a Malvern Zetasizer Nano ZS. A 30 μL aliquot of the microgel dispersion was placed onto a silicon substrate and characterized using the PeakForce QNM (Quantitative NanoMechanics) mode of the AFM (Veeco Metrology) after being dried at 50 °C for 2 hours. The microgels on the silicon substrate was sputter coated with a 5 nm homogeneous gold layer after being dried at 50 °C for 2 hours and observed by scanning electron microscopy (SEM, Hitachi S5500 FE-S(T)EM). A 30 μL aliquot of the microgel dispersion was placed onto carbon-coated cooper grids and was observed by transmission electron microscopy (TEM, JEOL 2100).

2.3 Preparation and characterization of Mickering emulsion

A 3 mL aliquot of the microgel dispersion (2 mg mL^{-1}) and 3 mL of oil (limonene) were mixed in a glass vial (15 mL) and emulsified using a vortex mixer for 1 min. 30 μL of the emulsion was placed in the wellplate and characterized using a confocal laser scanning microscope (CLSM, Zeiss LSM510 META MP). For easy

observation, the oil phase was dyed with a fluorescent NR, which was then excited using a 543 nm laser and the emission was detected from 565 to 615 nm. The microgels embedded with the green dye C7 were excited by a 488 nm argon ion laser and the emission was detected from 500 to 550 nm.

2.4 Preparation and characterization of colloidosomes

The as-formed Mickering emulsion in a microtube was stirred at a speed of 700 rpm. 3 mL aliquot of chitosan solution (1 wt% in 1 wt% acetic acid solution) was added dropwise into the emulsion. The reaction was carried out for 10 h. To purify the colloidosomes, the mixture was centrifuged at 4000 rpm for 5 min. This constrained the colloidosomes to the boundary of the oil and the aqueous phases. Consequently, the colloidosomes were added into ethanol to remove the oil core. Then, the colloidosomes were dropped onto a silicon wafer and were sputter-coated with a 5 nm homogeneous gold layer and characterized by FE-S(T)EM.

2.5 Load and release of model drug

FITC-Dex was selected as a model drug and loaded in the colloidosomes based on the method reported in the literature.[23] The colloidosomes were purified though dialysis in an ethanol/water mixture (1 : 1 v/v) for a week to remove the residue limonene. Afterwards, 10 mg of colloidosomes and 1 mL ($V_{Loading}$) of the FITC-Dex solution (0.5 mg mL^{-1}, $C_{Initial}$) were mixed for FITC-Dex loading on the shaking platform (300 rpm) for 36 h. The FITC-Dex-loaded colloidosomes were finally obtained *via* natural sedimentation. The concentration of the FITC-Dex ($C_{Supernatant}$) in the supernatant was evaluated using a fluorescence meter (The SpectraMax® i3x Platform). The FITC-Dex-loaded colloidosomes were then divided equally into three parts and dispersed into 5 mL ($V_{Release}$) of buffer solutions of pH = 4.0, 7.0 and 10.0, respectively. The fluorescence intensity of the buffer solution ($C_{Release}$) after 10 hours was measured using a fluorescence meter to determine the release of the FITC-Dex from the colloidosomes. The excitation wavelength for the fluorescence meter measurement was 488 nm and the detection wavelength was from 500 nm to 530 nm. The release of the FITC-Dex was calculated as a percentage according to release percentage $= C_{Release} \times V_{Release}/((C_{Initial} - C_{Supernate}) \times V_{Loading})$.

3 Results and discussion

3.1 Core–shell structured microgels

The microgels synthesized from the one-pot method are shown in Fig. 2. The as-formed core particles have spherical shapes and a narrow size distribution, as shown in Fig. 2a. The zeta-potential of the core particles is ~−52 mV, indicating that they are stable in the reaction system. After the addition of the shell monomers of NIPAM and AAc with MBA into the reaction, the P(NIPAM-*co*-AAc) were formed following the same polymerization mechanism with the core since both the core and shell monomers are derivatives of ethylene. At the same time, the PTFMA particles played a role as seeds for the nucleation of P(NIPAM-*co*-AAc), and thus led to core–shell microgels. Due to

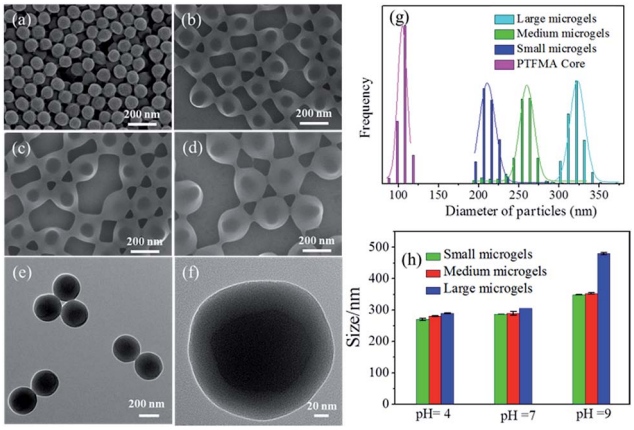

Fig. 2 The SEM morphology of (a) PTFMA particles and P(NIPAM-*co*-AAc)@PTFMA core–shell microgels with a mean size of (b) 212 nm, (c) 256 nm and (d) 323 nm. Typical TEM images of large microgels with (e) low and (f) high magnifications. (g) The size distribution from statistics of the SEM images of the above-mentioned particles, and (h) the hydrodynamic size of the P(NIPAM-*co*-AAc)@PTFMA core–shell microgels in buffered solutions at 25 °C.

the different interactions of PTFMA and P(NIPAM-*co*-AAc) with the electron beam, the core–shell structure of the microgels can be observed clearly in SEM (Fig. 2b–d) and TEM images (Fig. 2e and f). These images also confirm that the microgels have a spherical shape and uniform size. Fig. 2b–d and Fig. 2g demonstrate that the thickness of shell can be tuned by the amount of monomers added during the synthesis. This is because P(NIPAM-*co*-AAc) only grew on the PTFMA particles. The identical population of PTFMA makes the thickness of P(NIPAM-*co*-AAc) tunable by the amount of monomers that are used. This confirms that the PTFMA cores act as seeds in the synthetic process.

The size distribution of microgels from the statistics of the SEM images reflects the size of the microgels in the dry state, as shown in Fig. 2g. The diameter of the PTFMA particles (core particles) is 103 ± 5.8 nm. A series of core–shell microgels with a diameter of 212 ± 10.4, 256 ± 16.1 and 323 ± 10.2 nm was obtained after the introduction of the shell and thereafter named as small, medium and large microgels, respectively. The isoelectric points of these microgels are approximately at pH 4 (see ESI†). The hydrodynamic diameter of the microgels in solutions with different pHs are shown in Fig. 2h. The hydrodynamic diameters of all the samples increase with pH. The large microgels have a maximum expansion ratio (165%) on diameter from pH 4 to 9 compared to that of the medium and small microgels (129% and 125%). This results from the larger expansion of the thicker shell due to the electrostatic repulsion of the ionized carboxyl group (AAc) at high pH. It can be noted that the values of the hydrodynamic diameters of the small and medium microgels at each pH were close to each other, which was caused by the slight differences in the thicknesses of the shells (only 21.5 nm) where is the pH sensitivity function relies on.

The effects of the rigid cores on the mechanical properties of the microgels were studied by the QNM model of AFM. Fig. 3a

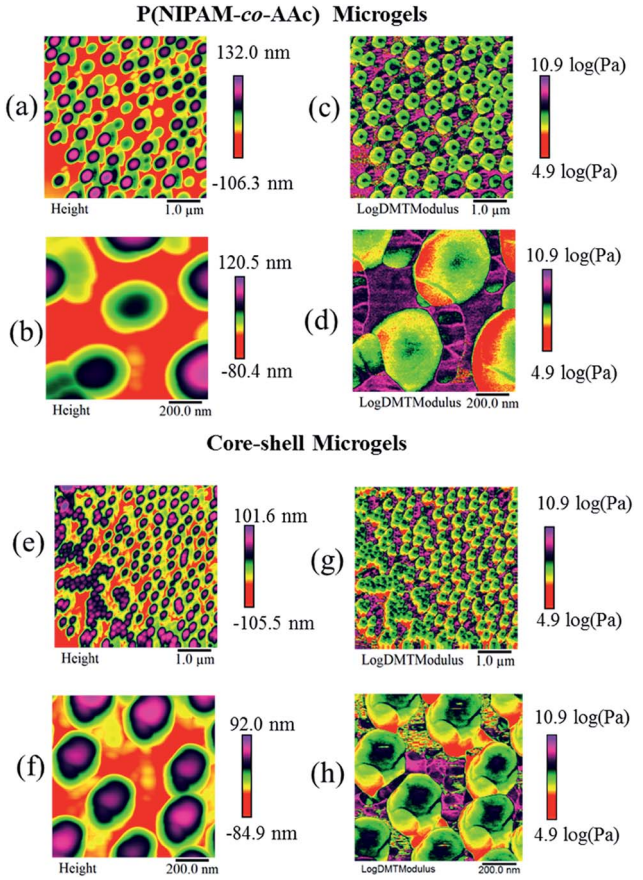

Fig. 3 The height (a, b, e and f) and log DMT modulus (c, d, g and h) map of the P(NIPAM-*co*-AAc) and P(NIPAM-*co*-AAc)@PTFMA microgels (large microgels) on silicon substrates.

and b show the height profile of the P(NIPAM-*co*-AAc) microgels (without PTFMA core). The elastic modulus map was calculated with the same resolution as the height map by fitting the retraction curve of the tip using the Derjaguin, Muller, Toporov (DMT) model[25] at each pixel and it is named as the DMT modulus. The distribution of the log of the DMT modulus of the P(NIPAM-*co*-AAc) microgels in Fig. 3c and d show a high agreement with the height distribution in Fig. 3a and b. The log of the DMT modulus of the P(NIPAM-*co*-AAc) microgel decreases with the distance to the center of the microgel because of the crosslinking density gradient from the center to the surface of the P(NIPAM-*co*-AAc) microgels,[26] wherein a higher crosslinking density of the polymer leads to a larger elastic modulus.[27] The core–shell microgels (Fig. 3g and h) show a similar trend for the modulus gradient but the high modulus region in the center is obviously larger than those without the PTFMA core, indicating that the mean modulus of the P(NIPAM-*co*-AAc) microgels is improved by the presence of the PTFMA core. The ratio between the height and area of the microgels from the height map was analyzed to determine their deformation on the silicon substrate. The ratio for the core–shell microgels is ~0.415, larger than that for the P(NIPAM-*co*-AAc) microgels (~0.275). It suggests that the rigid core significantly prevents the deformation of the microgels by enhancing its mechanical properties.

3.2 Mickering emulsion

After blending the microgel dispersion with limonene oil using a vortex mixer, the microgels assemble at the oil/water interface and form a Mickering emulsion. The CLSM images of the surface and cross-section of the emulsion droplets stabilized by large microgels are shown in Fig. 4a and b, respectively, wherein the microgels are labeled by dye C7 (green), whereas the oil by NR (red). The green dots are microgels arrayed at the oil/water interface in Fig. 4a. The red labeled oil phase can be recognized as a discontinuous phase in Fig. 4b, suggesting an as-formed oil-in-water emulsion. This indicates that the hydrophilic shell of the microgels, as an emulsion stabilizer, plays a dominate role compared to the hydrophobic core, because the hydrophilic particles usually lead to an oil-in-water emulsion, whereas the hydrophobic ones lead to the opposite.[10]

The selected area image from the CLSM (Fig. 4c) and its Fast Fourier Transform (FFT) image (Fig. 4d) show that the microgels form a hexagonal close packing (hcp) structure with a mean inter-particle space of ~302.1 nm. The value is even smaller than the diameter of the microgels in the dry state in SEM (~323 nm), proposing that the microgels might be compressed at the tangential plane of the oil droplet surface. However, it is against the observation and established theory[10,28] that the soft microgels spread as much as possible (stretched) at the interface to maximize the coverage area and thus minimize the direct contact between oil and water. The possible mechanism for this phenomenon is illustrated in Fig. 4i. As shown in Fig. 2e, most of the PTFMA cores are not at the geometrical center of the microgels. In the emulsion, the hydrophobic core tends to be in the oil solvent environment and thus forms the most thermodynamically favorable configuration of the microgels at the interface, as shown in Fig. 4i. The inter-particle distance calculation from the CLSM image is based on the fluorescent dye in the core. On one hand, the inter-core distance at the inner curve (dash line in Fig. 4i) is smaller than the microgels geometrical center distance at the outer curve (solid line in Fig. 4i). On the other hand, the hydrophilic shell swells more in the water side than in the oil side.

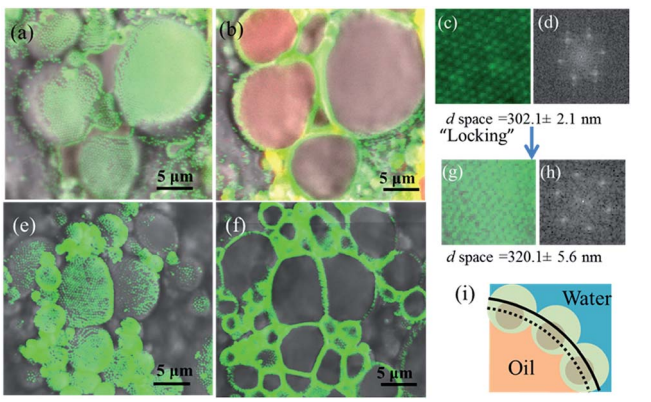

Fig. 4 The CLSM images of (a) surface, (b) cross-section of a Mickering emulsion, and (c) the selected area of the microgel arrays, and (d) its FFT image; (e–h) the corresponding results after the "locking" process by chitosan. (i) Illustration of the configuration of the microgels at the oil/water interface.

3.3 Colloidosomes based on core–shell microgels

The core–shell microgels are negatively charged. Therefore, chitosan as a natural cationic polyelectrolyte with an excellent biocompatibility was adopted to lock the microgels in the emulsion. Fig. 4e and f show the CLSM images of the Mickering emulsion after the addition of chitosan. The hcp structure of microgels at the interface (Fig. 4g) is still maintained after the "locking" process. However, the inter-particle distance increased to 320.1 nm, suggesting that chitosan was adsorbed and filled the inter-space among the microgels. Chitosan linked the microgels and led to the formation of the colloidosomes. Subsequently, ethanol was used to remove the oil and water phases of the emulsion and the colloidosomes were obtained after purification. As shown in Fig. 5a, typical colloidosomes exhibit a spherical morphology and aggregation of micron-sized polydispersed units. Fig. 5b shows the size of the colloidosomes ranging between 1 and 4 micrometres. The microgels merged with each other to form the walls of the colloidosomes. The microgels still maintain the hcp structure, which is in good agreement with the CLSM test. All the small (Fig. 5c), medium (Fig. 5d) and large (Fig. 5e) microgels were able to form the corresponding colloidosomes.

3.4 Model drug release

The permeability of the colloidosomes was investigated by a release test of the loaded FITC-Dex as a model drug. Fig. 6 shows the percentage of FITC-Dex release in different pH buffer solutions. It was found that the amounts of released drug increased

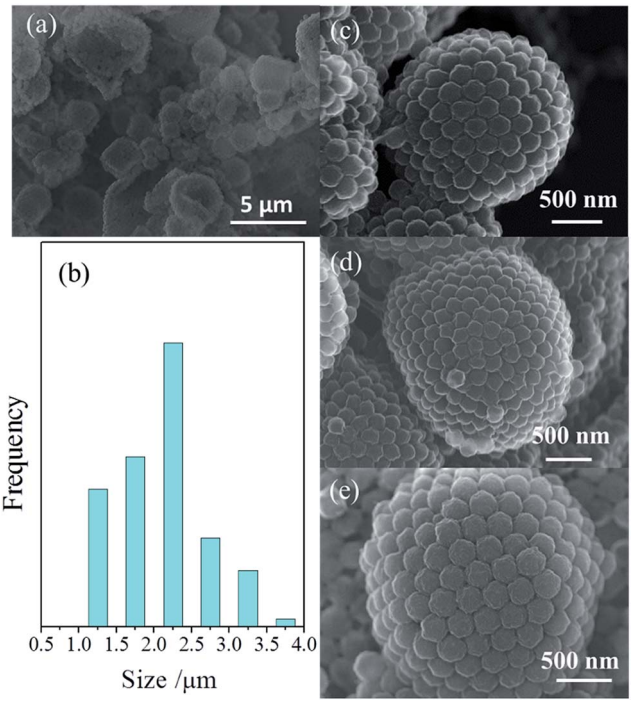

Fig. 5 The SEM images of the colloidosomes (a) after purification and their size distribution (b). Typical colloidosome made from small (c), medium (d) and large (e) microgels.

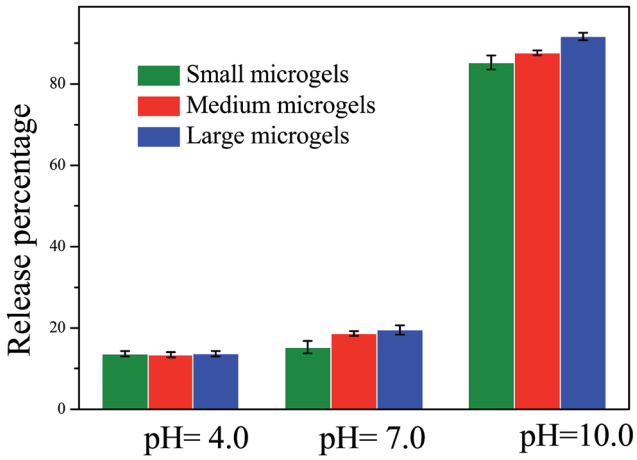

Fig. 6 The release of encapsulated FITC-Dex from the colloidosomes after 10 hours in media of different pHs.

with pH for all types of colloidosomes. Taking the colloidosomes from the small microgels as an example, the percentage of drug release increased from 13.63% to 85.23% when the pH changed from 4.0 to 10.0. This strong pH sensitivity can be a potential trigger for the release of the drug from the colloidosomes. This originates from the expansion of the microgels (the wall of the colloidosomes) at high pH (Fig. 2h), which increased the free volume of the polymer and promoted the diffusion of the FITC-Dex. This proves that the as-formed colloidosomes are responsive to pH and the permeability for the release of the drug can be coarsely controlled by changing the pH.

Comparison of the release profile of the colloidosomes formed from different sizes of microgels confirmed that permeability can be controlled by the thickness of the P(NIPAM-*co*-AAc) shells in high pH solutions. For example, the ratio of the shell thickness to the core diameter in small, medium and large microgels is ~1.0, 1.5 and 2.2, which corresponds to the percentage of the FITC-Dex released from the colloidosomes at 85.23% ± 1.7%, 87.62% ± 0.63% and 91.67% ± 0.91% at pH 10.0, respectively. The same trend was also found at pH 7. This is because the release of the drug from the polymer based materials follows the dissolution–diffusion model.[29] Due to their better solubility, the diffusion of hydrophilic molecules in the hydrophilic polymer was easier than that in the hydrophobic polymer.[30] The wall of colloidosomes was equivalent to the hydrophilic shell embedding hydrophobic core of microgels, as described in Fig. 1. The releases of the loaded FITC-Dex easily took place in the P(NIPAM-*co*-AAc) matrix but slowed down when the hydrophobic PTFMA was encountered. In this sense, the permeability of the colloidosomes can be fine-tuned by controlling the thickness ratio of the shell to core in the synthesis of the microgels.

It is noted that there was no obvious difference on the percentage of the release at pH 4.0. Because the colloidosomes were designed so that the release of the drug was triggered by a high pH value, the drug was supposed to be maintained in the colloidosomes at a low pH wherein fine control was not necessary.

4 Conclusions

The one-pot synthesis of core–shell structured P(NIPAM-*co*-AAc)@PTFMA microgels was developed. The rigid core improved the elastic modulus of the microgels and thus prevented the deformation of the microgels on the substrate. When assembling at the oil and water interface, the observed inter-particle distance of the microgels decreased, resulting from the eccentric core–shell structure. It was demonstrated that release of the loaded model drug FITC-Dex from as-formed colloidosomes can be coarsely adjusted by pH and finely tuned by the ratio of the shell to core size in the microgels. The dual-level permeability control offers great potential for precise drug release. Our findings provide insights into the design of multifunctional colloidosomes for biomedicine.

Acknowledgements

This study was supported by the Research Council of Norway (RCN) by the PETROMAKS2 project FP project SustainCem (Grant No. 228599) and RCN, Det Norske Oljeselskap ASA and Wintershall Norge AS by the NANO2021 KPN project WINPA (Grant No. 234626). We would like to thank Sulalit Bandyopadhyay (Ugelstad Laboratory, NTNU) for the zeta-potential and hydrodynamic diameter measurements.

References

1 G. Verma and P. Hassan, *Phys. Chem. Chem. Phys.*, 2013, **15**, 17016–17028.
2 P. H. Keen, N. K. Slater and A. F. Routh, *Langmuir*, 2011, **28**, 1169–1174.
3 Y. Gong, A. M. Zhu, Q. G. Zhang, M. L. Ye, H. T. Wang and Q. L. Liu, *ACS Appl. Mater. Interfaces*, 2013, **5**, 10682–10689.
4 T. Bollhorst, S. Shahabi, K. Wörz, C. Petters, R. Dringen, M. Maas and K. Rezwan, *Angew. Chem., Int. Ed.*, 2015, **127**, 120–125.
5 W. Cao, R. Huang, W. Qi, R. Su and Z. He, *ACS Appl. Mater. Interfaces*, 2014, **7**, 465–473.
6 Y. Zhao, Z. Chen, X. Zhu and M. Möller, *J. Mater. Chem. A*, 2015, **3**, 24428–24436.
7 Z. Wang, M. van Oers, F. P. Rutjes and J. van Hest, *Angew. Chem., Int. Ed.*, 2012, **51**, 10746–10750.
8 Z. Wang, M. van Oers, F. P. Rutjes and J. van Hest, *Angew. Chem.*, 2012, **124**, 10904–10908.
9 A. Dinsmore, M. F. Hsu, M. Nikolaides, M. Marquez, A. Bausch and D. Weitz, *Science*, 2002, **298**, 1006–1009.
10 W. Richtering, *Langmuir*, 2012, **28**, 17218–17229.
11 V. D. Gordon, X. Chen, J. W. Hutchinson, A. R. Bausch, M. Marquez and D. A. Weitz, *J. Am. Chem. Soc.*, 2004, **126**, 14117–14122.
12 R. K. Shah, J.-W. Kim and D. A. Weitz, *Langmuir*, 2009, **26**, 1561–1565.
13 Y. Gong, A. M. Zhu, Q. G. Zhang and Q. L. Liu, *RSC Adv.*, 2014, **4**, 9445–9450.
14 W. Wang, A. H. Milani, L. Carney, J. Yan, Z. Cui, S. Thaiboonrod and B. R. Saunders, *Chem. Commun.*, 2015, **51**, 3854–3857.
15 J.-W. Kim, A. Fernández-Nieves, N. Dan, A. S. Utada, M. Marquez and D. A. Weitz, *Nano Lett.*, 2007, **7**, 2876–2880.
16 B. R. Saunders, N. Laajam, E. Daly, S. Teow, X. Hu and R. Stepto, *Adv. Colloid Interface Sci.*, 2009, **147**, 251–262.
17 L. Isa, F. Lucas, R. Wepf and E. Reimhult, *Nat. Commun.*, 2011, **2**, 438.
18 M. Kirigakubo, *J. Oral. Maxillofac. Surg.*, 1986, **32**, 20.
19 S. M. Hashmi and E. R. Dufresne, *Soft Matter*, 2009, **5**, 3682–3688.
20 A. San Miguel and S. H. Behrens, *Soft Matter*, 2011, **7**, 1948–1956.
21 B. Samanta, D. Patra, C. Subramani, Y. Ofir, G. Yesilbag, A. Sanyal and V. M. Rotello, *Small*, 2009, **5**, 685–688.
22 E. Yoshida, *Colloid Polym. Sci.*, 2012, **290**, 525–530.
23 O. J. Cayre, J. Hitchcock, M. S. Manga, S. Fincham, A. Simoes, R. A. Williams and S. Biggs, *Soft Matter*, 2012, **8**, 4717–4724.
24 D. Go, T. E. Kodger, J. Sprakel and A. J. Kuehne, *Soft Matter*, 2014, **10**, 8060–8065.
25 B. V. Derjaguin, V. M. Muller and Y. P. Toporov, *J. Colloid Interface Sci.*, 1975, **53**, 314–326.
26 M. Stieger, W. Richtering, J. S. Pedersen and P. Lindner, *J. Chem. Phys.*, 2004, **120**, 6197–6206.
27 Z. Wang, A. A. Volinsky and N. D. Gallant, *J. Appl. Polym. Sci.*, 2014, **131**, 41050.
28 K. Geisel, L. Isa and W. Richtering, *Langmuir*, 2012, **28**, 15770–15776.
29 M. I. Cabrera, J. A. Luna and R. J. Grau, *J. Membr. Sci.*, 2006, **280**, 693–704.
30 B. Jeong, Y. H. Bae and S. W. Kim, *J. Controlled Release*, 2000, **63**, 155–163.

